From quadrupedal to bipedal walking ‘on the fly’: the mechanics of dynamical mode transition in primates

Peter Aerts, Jana Goyens, Gilles Berillon, Kristiaan d’Août, François Druelle

© 2023. Published by The Company of Biologists Ltd | Journal of Experimental Biology (2023) 226, jeb244792. doi:10.1242/jeb.244792

RESEARCH ARTICLE

From quadrupedal to bipedal walking 'on the fly': the mechanics of dynamical mode transition in primates

Peter Aerts[1,2,*], Jana Goyens[1], Gilles Berillon[3,4], Kristiaan D'Août[5] and François Druelle[1,3,4]

ABSTRACT

We investigated how baboons transition from quadrupedal to bipedal walking without any significant interruption in their forward movement (i.e. transition 'on the fly'). Building on basic mechanical principles (momentum only changes when external forces/moments act on the body), insights into possible strategies for such a dynamical mode transition are provided and applied first to the recorded planar kinematics of an example walking sequence (including several continuous quadrupedal, transition and subsequent bipedal steps). Body dynamics are calculated from the kinematics. The strategy used in this worked example boils down to: crouch the hind parts and sprint them underneath the rising body centre of mass. Forward accelerations are not in play. Key characteristics of this transition strategy were extracted: progression speed, hip height, step duration (frequency), foot positioning at touchdown with respect to the hip and the body centre of mass (BCoM), and congruity between the moments of the ground reaction force about the BCoM and the rate of change of the total angular moment. Statistical analyses across the full sample (15 transitions of 10 individuals) confirm this strategy is always used and is shared across individuals. Finally, the costs (in J kg^{-1} m^{-1}) linked to on the fly transitions were estimated. The costs are approximately double those of both the preceding quadrupedal and subsequent bipedal walking. Given the short duration of the transition as such (<1 s), it is argued that the energetic costs to change walking posture on the fly are negligible when considered in the context of the locomotor repertoire.

KEY WORDS: Terrestrial locomotion, Primates, Locomotor mechanics, Quadrupedal–bipedal transitions, *Papio anubis*

INTRODUCTION

Bipedal and quadrupedal locomotion share common biomechanical features in non-human primates and might be controlled by the same basic neuromotor mechanism (for an elaborate discussion on this, see Aerts et al., 2000; D'Août et al., 2004; Druelle et al., 2017a; Higurashi et al., 2019; Nakajima et al., 2004, 2001; Zehr et al., 2009). Also, the coordination between forelimbs (arms) and hindlimbs (legs) in (habitual) bipedal humans is suggested to be the result of the same coupled pattern generators as observed in habitual quadrupeds (Balter and Zehr, 2007; Dietz, 2002; Dietz et al., 2001; Zehr et al., 2009). In this context, it has been hypothesized that the components of the quadrupedal neural circuitry were conserved during the evolution of hominins and used for bipedal locomotion (Zehr et al., 2009). The use of the same neural network would have greatly facilitated the evolutionary transition from quadrupedal animals to bipedal ones. Nevertheless, an evolutionary transition from a quadrupedal ancestor to a habitual bipedal primate probably requires intermediate forms capable of both locomotor modes (Rose, 1991).

Interestingly, all extant Catarrhini species, while largely relying on the quadrupedal locomotor system, are also capable of occasional bipedal walking and use this locomotor mode spontaneously in their daily activities (e.g. Druelle and Berillon, 2014; Rosen et al., 2022). The proportion of their bipedal walking has been widely quantified in natural (Carvalho et al., 2012; Hunt, 1994; Rose, 1976; Stanford, 2006; Wrangham, 1980) and experimental contexts (Druelle et al., 2016; Videan and McGrew, 2001, 2002), and also the kinematics of bipedalism in non-human primates has been studied extensively (e.g. Aerts et al., 2000; Berillon et al., 2010; Blickhan et al., 2018, 2021; Demes, 2011; Hirasaki et al., 2004; Nakatsukasa et al., 2006; Ogihara et al., 2010; Thompson et al., 2015, 2021; for an overview, see Druelle et al., 2022a). Nevertheless, little is known about how primates (or quadrupeds in general) deal with dynamic transitions from quadrupedal to bipedal walking 'on the fly', such as for instance exemplified in Fig. 1A. Nakajima et al. (2001) mentioned that *Macaca fuscata*, at least, can move from quadrupedal to bipedal walking without any break in their forward speed. Apparently, baboons are also capable of this (Fig. 1A).

The exploitation of such behavioural capacity might have been essential in the evolutionary emergence of habitual bipedalism in hominins. From this point of view, it is important to better understand the mechanics of quadrupedal–bipedal transitions on the fly.

In this context, we investigated the mechanics of on the fly quadrupedal–bipedal transitions in the olive baboon, *Papio anubis*. We chose to focus on this species because it can be considered, among primates, a terrestrially specialized quadruped, frequently showing transitions toward bipedalism in its natural movement repertoire (e.g. Berillon et al., 2010; Druelle et al., 2022b; Rose, 1976). We first provide a theoretical framework that considers the mechanical options available for a quadruped to perform on the fly transitions, relating the whole-body level to kinematical and dynamical strategies. Preliminary, qualitative observations of the transitions performed by several specimens of the study population led us to hypothesize that they all, and always, make the transition in a very similar way (i.e. they use the same basic strategy). In order to test this, we first describe in detail, relying on the theoretical framework, the transition mechanics in play for one worked example (containing several quadrupedal steps, the transition and several bipedal steps in

[1]Laboratory of Functional Morphology, University of Antwerp, 2610 Antwerp, Belgium. [2]Department of Movement and Sports Sciences, University of Ghent, 9000 Ghent, Belgium. [3]HNHP (UMR 7194), CNRS-MNHN-UPVD, 75116 Paris, France. [4]Primatology Station of the CNRS (UAR 846), 13790 Rousset, France. [5]Institute of Life Course and Medical Sciences, University of Liverpool, Liverpool, L7 8TX, UK.

*Author for correspondence (peter.aerts@uantwerpen.be)

P.A., 0000-0002-6867-5421; J.G., 0000-0003-0176-884X

Received 19 July 2022; Accepted 30 November 2022

Journal of Experimental Biology (2023) 226, jeb244792. doi:10.1242/jeb.244792

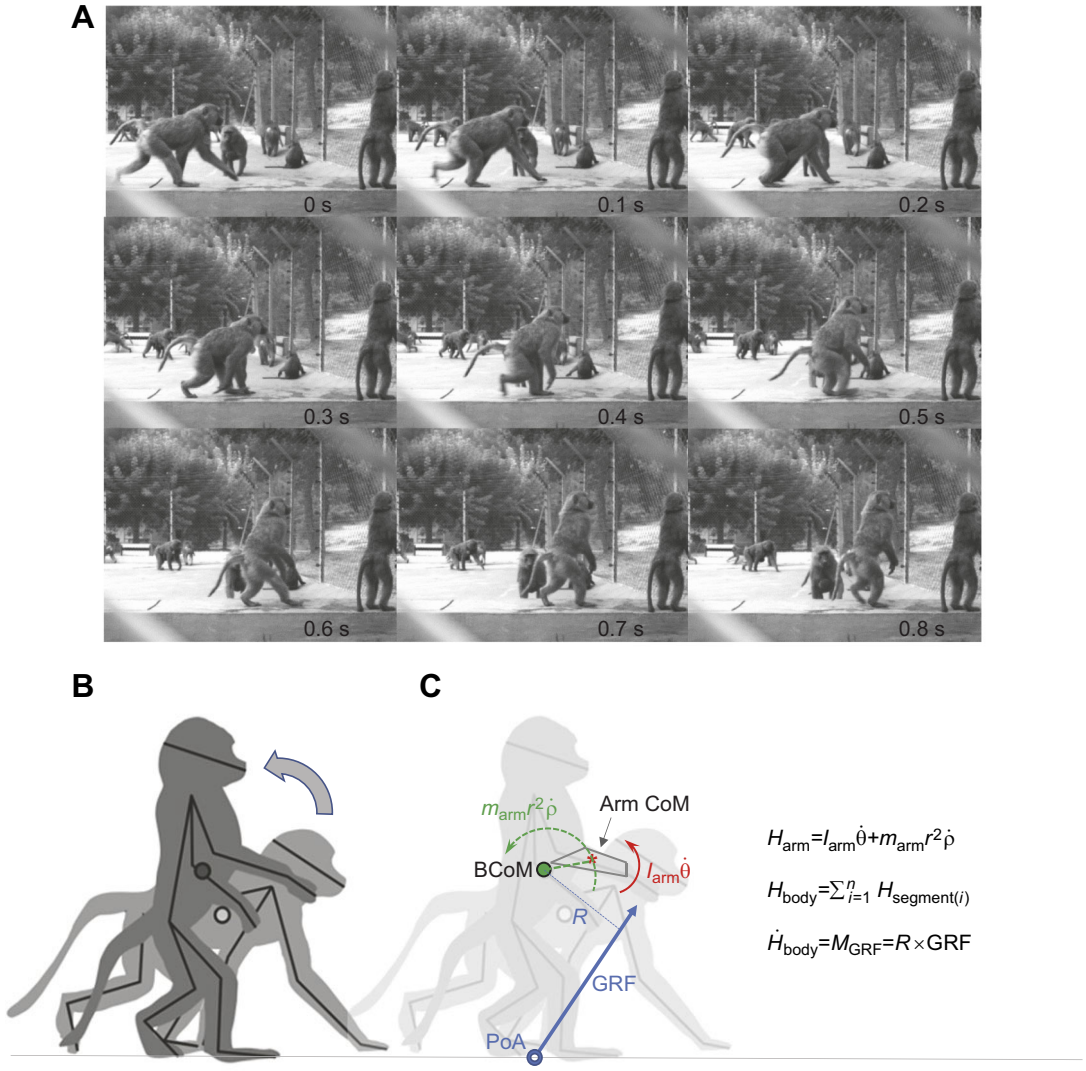

Fig. 1. 'On the fly' quadrupedal–bipedal transition. (A) Representative illustration of a quadrupedal–bipedal transition 'on the fly' in a walking sequence of a baboon. (B) Outlines of the start and end posture of a quadrupedal–bipedal transition on the fly. (C) The angular momentum of the total body (H_{body}) is the sum of the angular momenta of all segments; each segmental angular momentum (for instance, H_{arm} for the lower arm) equals the sum of its local ($I_{arm}\dot{\theta}$) and its remote ($m_{arm}r^2\dot{\rho}$) term; $\dot{H}_{body}$ (instantaneous change of H_{body}) equals the moment of the ground reaction force ($R\times GRF=M_{GRF}$) [where I_{arm} is the moment of inertia of the arm about its centre of mass (CoM; red asterisk), $\dot{\theta}$ is the instantaneous angular velocity of the arm about its CoM, m_{arm} is arm mass, r is the instantaneous distance from Arm CoM to body CoM (BCom), $\dot{\rho}$ is instantaneous angular velocity of Arm CoM about BCoM, GRF is the ground reaction force, R is the moment arm GRF about BCoM, and PoA is the point of application of GRF].

sequence) and then define the kinematical and dynamical key characteristics of the transition. As a last step, we establish how stereotyped the strategy is across individuals by statistically assessing and discussing the variability of key characteristics. We thus provide insights into the control strategy used by the baboons to lift the heavy upper body (head–arms–trunk or HAT; ∼75% of body weight) in an orthograde posture during walking. We hypothesize that (1) the transition from quadrupedal to bipedal locomotion is effectively performed on the fly, i.e. in a smooth and non-erratic way and without any significant interruption in forward movement. Further, we hypothesize that (2) all individuals use a similar strategy and that, given the spontaneous nature of bipedal behaviours in baboons, (3) the transition can be performed in an efficient way, i.e. implying limited extra costs and efforts compared with the normal quadrupedal and bipedal locomotion. When confirmed, this last hypothesis supports the above-mentioned point of view on the evolutionary importance of on the fly transitions in the locomotor repertoire of extinct primates (and potentially in Miocene apes and early hominins).

MATERIALS AND METHODS

Theoretical framework

Straightforward mechanical considerations provide a way to analyse and interpret the dynamics of on the fly quadrupedal–bipedal transitions of quadruped animals as exemplified in Fig. 1A. These transitions are characterized by, principally, sagittal plane kinematics and involve considerable reorientation of body segments, mostly represented in the upwards rotation of the heavy HAT segment (Fig. 1B). This implies considerable changes in the total 'amount of rotational movement' (i.e. angular momentum) of the body (H_{body}; see Fig. 1C). Expressed with respect to the origin of a frame of reference moving with the body centre of mass (BCoM; see Fig. 1C), the quadrupedal–bipedal on the fly transition

Journal of Experimental Biology (2023) 226, jeb244792. doi:10.1242/jeb.244792

can thus be expected to result in a sudden and temporary rise of H_{body} above its normal oscillations about zero during steady walking.

According to basic mechanical principles, angular momentum can only change as a result of external moments acting on the multi-segmented body. Consequently, in the frame of reference moving with the BCoM, the time derivative (instantaneous change) of H_{body} ($=\dot{H}_{body}$; see Fig. 1C) equals, at any instant, the resultant external moment of the total body ground reaction force (GRF; see Fig. 1C) about the BCoM [air resistance can safely be neglected (small compared with the GRFs), and all moments of the segmental weights (mass times acceleration due to gravity, mg) and of the segmental fictitious forces as a result of the BCoM accelerations sum to zero]. When walking steadily quadrupedally or bipedally, $\dot{H}_{body}$ must fluctuate in a regular way about zero. Hence, the pattern of the moment of the GRF about the BCoM is regular, too. However, upon the on the fly quadrupedal–bipedal transition, this regularly fluctuating pattern becomes disrupted. This must be reflected in alterations of the GRF in terms of position and/or orientation and/or magnitude, as the moment of the GRF about the BCoM can only change over time in two (mostly coupled) ways: (i) variation of the magnitude of the GRF and/or (ii) variation of its moment arm (R; see Fig. 1C) by either a shift of the point of application (PoA) of the GRF relative to the BCoM and/or by the reorientation of the GRF vector (Fig. 2A–C). However, position, magnitude and orientation of the GRF are the net representation of all instantaneous (loco-)motor actions by the animal. Therefore, studying the temporary changes of the moment of the GRF about the BCoM and interpreting these in terms of the observed kinematics and dynamics of the body segments can provide insights into the transition dynamics and the underlying control strategies.

On the fly transition implies upwards acceleration of the heavy HAT from its initial pronograde posture. $\dot{H}_{body}$ can thus be expected to show (in the reference frame as in Fig. 2A–C) a positive peak. However, towards the end of the transition, the upwards rotating heavy HAT must be decelerated again (i.e. negative $\dot{H}_{body}$) in order to reach a stable orthograde posture. Consequently, during the transition, the initial counterclockwise moment (in the reference frame as in Fig. 2A–C) of the GRF must rapidly flip over into a clockwise one. This happens when the line of action of the GRF changes from being in front of the BCoM to running behind the BCoM, which can be realized by (a combination of) (i) shifting the

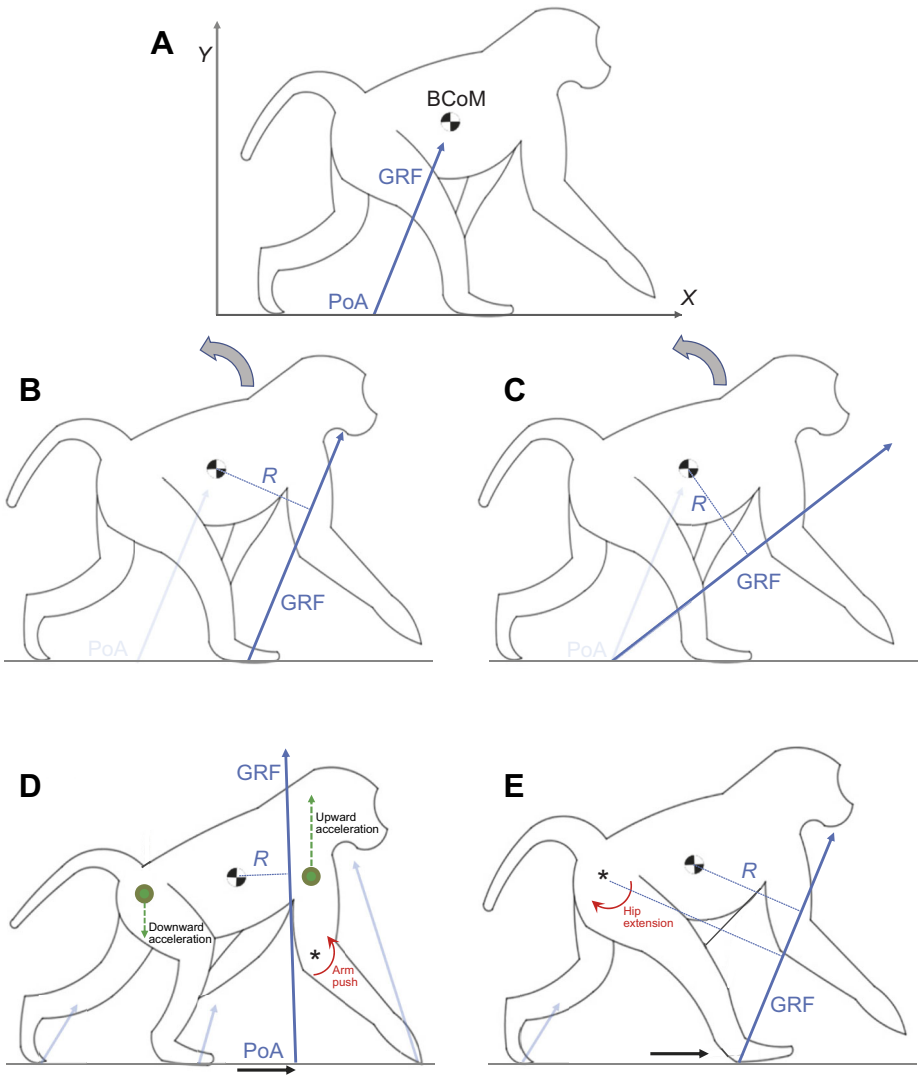

Fig. 2. Imaginary 'stills' from a walking sequence of a quadruped. (A) In the conditions applying at the instant shown here, GRF has no moment about the BCoM (hence $\dot{H}_{body}$=0). (B,C) To generate a counterclockwise moment (hence $\dot{H}_{body}$>0), the PoA can be shifted forward (B) and/or GRF can be oriented more horizontally (C). Larger moments can further be realized by increasing the amplitude of GRF (C). Similar, but opposite shifts and reorientations result in a clockwise moment (hence $\dot{H}_{body}$<0). (D,E) Options to generate a counterclockwise moment about the BCoM during the early quadrupedal bipedal transition 'on the fly' when still on all fours (D) and when the fore limbs have lost contact with the ground (E). Abbreviations as in Fig. 1; see Materials and Methods and Results and Discussion sections for more explanation; asterisks represent joint rotation centres.

Journal of Experimental Biology (2023) 226, jeb244792. doi:10.1242/jeb.244792

PoA and (ii) redirecting the line of action of the GRF (more horizontally or vertically; Fig. 2A–C). Both affect the length of the moment arm *R*, and hence also the magnitude of the moment itself. Clearly, these time fluctuations of the moments of the GRFs (in terms of varying magnitude, orientation and position) are most likely not the control measures the neuromotor system is directly aiming at. However, they do reflect the underlying motor strategy used to carry out the quadrupedal–bipedal on the fly transition.

Let us focus on the upwards acceleration phase of the HAT first. As long as forelimbs and hindlimbs are in contact with the ground simultaneously, the PoA can be moved forward with respect to the BCoM by redistributing the vertical loads taken by the hands and feet (i.e. more load at the forelimbs). Changes in the horizontal loads by the hand or feet do not affect the PoA. Higher relative hand loading may result from actively pushing the front parts upwards, while lower relative loading at the feet can be realized by a downward acceleration of the hind parts (‘dropping the hind parts’; Fig. 2D). Theoretically, this may happen without affecting the magnitude and orientation of the total GRF (i.e. when this redistribution is such that it does not change the acceleration, in magnitude and direction, of the BCoM). More likely, however, this total GRF will also change because of the combined limb action and if this goes along with an increase in its propulsive component (forward acceleration) and/or its vertical component (upward acceleration), an additional positive effect on the counterclockwise pitching moment will be the result (larger magnitude and larger *R*). Notice that, in a quadrupedal posture, lowering the hind parts will automatically cause the trunk to be more erect.

However, inherent to the quadrupedal–bipedal transition, hands lose contact with the ground soon, and keeping the PoA in a more anterior position thus readily requires putting down the feet further forward (‘foot repositioning’; Fig. 2E). As a result, hind parts may drop to some extent as well, but more important is that (especially early in the single limb stance) hip extensors must contract forcefully to counter the increased moment of the GRF about the hip (Fig. 2E). Such strong hip extensor activity supports HAT accelerations. Obviously, this will be reflected in the magnitude and orientation of the GRFs, too.

As mentioned, at the end of the transition, the heavy HAT must decelerate in order for H_{body} to oscillate about zero again during the subsequent steady bipedal walking. It seems very plausible that this deceleration largely results from the gravitational forces acting on the heavy HAT, if needed assisted by subtle reversed actively controlled strategies: reduced forward positioning of the feet (affecting PoA) and stronger hip flexor activity at the end of limb retraction (affecting the GRF at the end of stance). Inevitably, however, this will be reflected in the pattern of the moment of the GRF about the BCoM.

From the above it must be obvious that, whether still on all fours or already bipedal, creating upward momentum of the HAT can go along with temporarily increased horizontal, forward-directed GRFs, and hence with temporary forward acceleration of the BCoM. This observation is important for two reasons. Firstly, overall whole-body acceleration during forward locomotion as such can purposely be applied as a strategy to make the on the fly transition (compare to a motorcycle ‘wheely’ when forcefully accelerating; see Druelle et al., 2022a). Such whole-body acceleration probably explains bipedal running bouts in lizards (Aerts et al., 2003) and probably also in the stiff-bodied cockroaches (Full and Tu, 1991). Mechanistically, however, within the locomotor cycles, this will always be reflected in kinematical and dynamical phenomena as previously described. Secondly, (temporary) forward acceleration of the BCoM, if present, inevitably implies upward pitching of the body and less grip by the forelimbs on the ground (Aerts et al., 2003; Druelle et al., 2022a). This, together with the fact that the forelimbs readily lose ground contact during transition anyway, suggests that the role of the forelimbs in the on the fly transition is probably limited.

Experimental design

At the Technical Platform of Motion Analysis of Primates (MAP, Primatology Station of the CNRS, Rousset sur Arc, France; e.g. Anvari et al., 2014; Berillon et al., 2010), we collected data on quadrupedal–bipedal walking transitions performed on the fly by olive baboons, *Papio anubis* (Lesson 1827). One Baumer HXC13 digital camera recorded the sagittal kinematics of the animals at 200 Hz while walking unrestrained on a 6 m long walkway (see Fig. 1A). This observational protocol ensures natural, voluntary and spontaneous behaviour. We also positioned a mirror at the end of the walkway because we observed that it stimulated their bipedal behaviour, thus allowing us to record quadrupedal–bipedal transitions in the field of view of the camera. Animals approached the mirror, and by us tilting the mirror backwards during the approach, baboons (often) made the quadrupedal–bipedal transition proceeding upright on the hindlimbs. Ideally, (single limb) GRFs of the entire transition (quadrupedal steps+transition steps+bipedal steps) should be available. One force plate was built into the walkway; hence, GRFs could be recorded only occasionally (because animals were walking unrestrained and unconditioned along the track), and logically never for the required series of sequential steps. It will be shown, however, that for the present purpose, GRFs and PoAs can reliably be calculated, making this methodology potentially suitable for video recordings made in the field. Fig. 1A shows a representative series of stills taken from our lateral camera. Experiments were approved by the Regional Ethical Committee for animal experimentation of the Midi-Pyrénées Region (Letter MP/01/15/02/08).

The study group consisted of 60 individuals ranging from newborn infants to adults. From the screening of all recorded sequences, 15 could finally be retained for further analysis. Selection criteria were: (1) uninterrupted walking along the walkway including a quadrupedal–bipedal transition, and (2) no other animal obscuring the view. These 15 sequences belonged to 10 individuals ranging from 2.85 to 16.12 kg (Table 1).

Frame by frame, 25 body points were digitized (at 200, 100 or 50 Hz, depending the locomotor speed and cycling frequency of the specimens), defining 15 body segments: head [+ neck; nostrils, back

Table 1. Individual information

ID	Name	Mass (kg)	Age (years)*	Sex	No. sequences digitized
V916F	Babar	16.12	4.9	M	1
V936G	Fleur	2.85	0.78	F	3
V902G	Céline	7.62	3.81	F	1
V792BA	Chris	10.33	4.02	M	1
V896BB	Dédé	7.26	2.95	M	4
V792BB	Dictée	6.37	2.23	F	1
V936H	Emeraude	5.45	2.03	F	1
V916J	Filosophie	3.59	1.16	F	1
V908GA	Epine	5.86	2.18	F	1
V936D	Ursuline	14.08	7.62	F	1

*If more than one sequence was digitized for an individual, we took the mean age of the individual across all the sequences used in the sample.

of the head (occiput), eyebrows], trunk [extremity of the tail, base of the tail (sacral vertebrae 3), base of the neck (cervical vertebrae 7)], arm, forearm and hand (left: tip of the 3rd finger, wrist joint and elbow; right: tip of the 3rd finger, metacarpophalangeal joint, wrist joint, elbow, acromion), thigh, shank and foot [left: tip of the 3rd toe, medial malleolus, heel (tuber calcanei), knee joint; right: tip of the 3rd toe, metatarsophalangeal joint, tarsometatarsal joint, lateral malleolus, heel (tuber calcanei), knee joint, greater trochanter; see Berillon et al., 2010]. As animals could not be marked, the digitization was more sensitive to noise. Therefore, after the calibration, the raw (position) data were filtered at 7 Hz in Matlab (zero phase shift, fourth-order Butterworth filter; Matlab version R2018b, The MathWorks, Natick, MA, USA).

Linear measures of segmental dimensions were available for all individuals (or for individuals of similar sex and size for Filosophie and Ursuline) used in the present analysis. These data were used as input for geometric modelling (based on Crompton et al., 1996; Druelle et al., 2017b) to obtain for each segment the mass, the relative position of the centre of mass (CoM) along the segment's long axis and with respect to the proximal end, and the moment of inertia about the frontal axis at the level of the segment's CoM (Table S1).

It must be noticed that shoulder and hip positions could only be digitized at the camera-side of the animals, meaning that effects of pelvic and pectoral rotations on the planar projection of these markers at the opposite side are not taken into account. Yet, the effects on the position of the contralateral hip and shoulder are probably small. Girdle rotations up to ±15 deg away from the transversal axis result in deviations in hip and shoulder position of maximally 3.5% of the pelvic and pectoral widths, respectively. Still, it is worth mentioning that this may somewhat influence the planar projection length, as well as the estimated angular position, of the thigh and upper arm at the opposite side of the animal, and hence also to some extent the position of the CoM of these elements. In this way, this simplification will affect the calculations as mentioned in the next section. However, given that position errors can safely be expected to be small (see above) and given that the thigh and upper arm only take together less than 10% of the body mass, the potential errors introduced in this way are assumed to be negligible in the context of present conceptual planar approach.

Data handling

Using these individual morphometrical data and the coordinates of the digitized body points, the position of the BCoM was obtained in each frame as follows:

$$\mathrm{BCoM}_{x,y} = \sum_1^{15} m_i x_i, y_i \Big/ \mathrm{bm}, \quad (1)$$

where $\mathrm{BCoM}_{x,y}$ is the x,y coordinates of the BCoM, m_i is the mass of segment m_i is the mass of segment i and x_i,y_i is the coordinates in the sagittal plane of the CoM of segment i, and bm is the total body mass of the individual. First and second (numerical) time derivatives of the position of the BCoM in the sagittal plane (Euler differentiation) yielded the instantaneous velocities (BCȯM) and accelerations (BCö M).

The actual quadrupedal–bipedal transition was determined on the basis of the vertical position and velocity of the BCoM. First, the step(s) during which the BCoM shifts upwards were identified. The start of the transition time interval is set when the vertical BCoM velocity ($\mathrm{BC\dot{o}M}_y$) becomes positive; the end when this velocity drops below zero again (see Fig. 3A).

The average walking speed of the transition bouts (quadrupedal+transitional+bipedal steps) was obtained from the slope of the linear regression of the forward displacement of the BCoM against time (see Fig. 3B). The steadiness of walking throughout the transition was assessed on the basis of the R^2-value of this regression. The closer to 1 it is, the more steady the transition bout is.

Magnitude and orientation of the GRF are given by:

$$\mathrm{GRF}_x = \mathrm{BC\ddot{o}M}_x\ \mathrm{bm}, \quad (2)$$

$$\mathrm{GRF}_y = (\mathrm{BC\ddot{o}M}_y + \boldsymbol{g})\mathrm{bm}. \quad (3)$$

Segmental orientation regarding the horizontal axis was calculated for each frame and the first time derivative of this angle provides the angular velocity $\dot{\theta}$ of each segment about its own CoM (see also Fig. 1C). The position of the CoM of each segment with regard to the BCoM can be expressed in polar coordinates (r, ρ; see Fig. 1C). The first time derivative of the angular coordinate ($\dot{\rho}$) represents the angular velocity of the segmental CoM about the BCoM (Fig. 1C). These data enable calculation of the total angular momentum of the body (H_{body}) and its instantaneous rate of change ($\dot{H}_{\mathrm{body}}$) (for equations, see Fig. 1C). Knowing $\dot{H}_{\mathrm{body}}$ and the magnitude and orientation of GRF, the PoA of the GRF (with respect to the BCoM) can be calculated as:

$$\mathrm{PoA} = \frac{\dot{H}_{\mathrm{body}} - \mathrm{GRF}_x\ \mathrm{BCoM}_y}{\mathrm{GRF}_y}. \quad (4)$$

This position can afterwards be recalculated with respect to any other (body)point provided the latter's position regarding the BCoM is known.

We calculated the instantaneous mechanical energy for each segment, as follows:

$$E_i = m_i \boldsymbol{g} y_i + \frac{m(\dot{x}_i^2 + \dot{y}_1^2)}{2} + \frac{I_i \dot{\theta}_i^2}{2}, \quad (5)$$

where m_i is the mass of segment i, $\boldsymbol{g}$ is the gravitational acceleration (9.81 m s^{-2}), y_i is the instantaneous height of the CoM of segment i, $\dot{x}_i$ *and* $\dot{y}_i$ are the linear velocity of the segment CoM and $\dot{\theta}_i$ is the angular velocity of the segment i in the sagittal plane. The time differential of the energy yielded the instantaneous power fluctuations for each segment.

To obtain maximized estimates for the costs of the transition, we assumed that no energy transfer happens between segments and that no elastic recovery occurs. In other words, all mechanical energy input and dissipation come at the expense of muscle activation (notice that actual costs will probably be smaller because of some energy transfer and elastic recovery). For power input (i.e. positive power or energy rate), an efficiency (mechanical power/metabolic power) of 0.25 is assumed; for negative power (dissipation), the efficiency is −1 (e.g. Alexander, 2003). In this way, instantaneous metabolic power is calculated per segment and then summed over all segments. The time integral of this total instantaneous power yields an estimate of the metabolic energy costs for the considered time interval. To determine the transition costs, the coinciding time interval is determined on the basis of BCoM_y: during the upwards movement, this velocity is positive and the zero-crossings of the velocity profile determine the start and end of the transition (see above and Fig. 3A). The time integral of the power profile for an identical time interval just prior to and immediately following the transition is used as an estimate for the corresponding quadrupedal and bipedal walking costs, respectively. It is important to note that in this way only the metabolic costs to do mechanical work are taken

Journal of Experimental Biology (2023) 226, jeb244792. doi:10.1242/jeb.244792

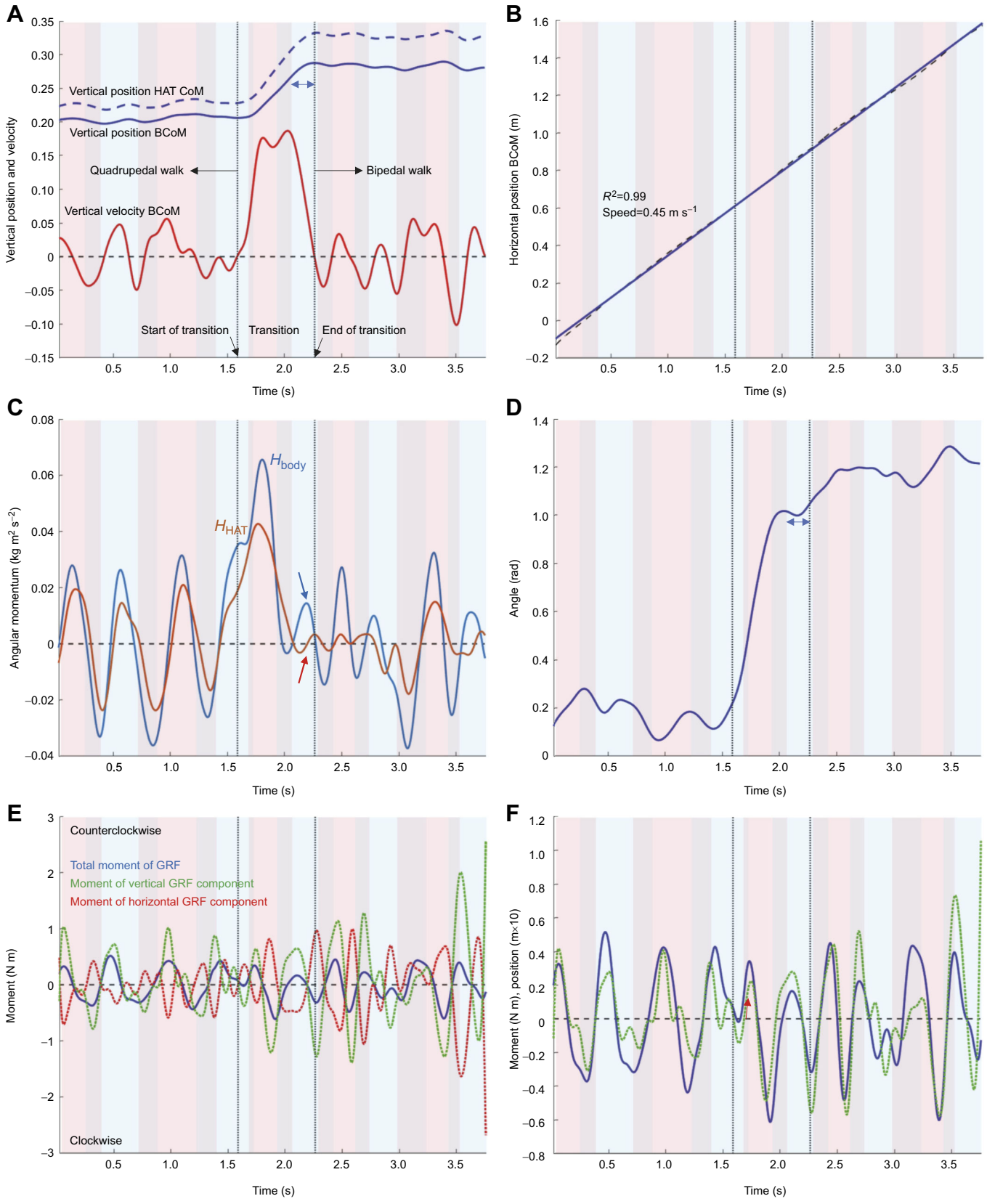

Fig. 3. See next page for legend.

Journal of Experimental Biology (2023) 226, jeb244792. doi:10.1242/jeb.244792

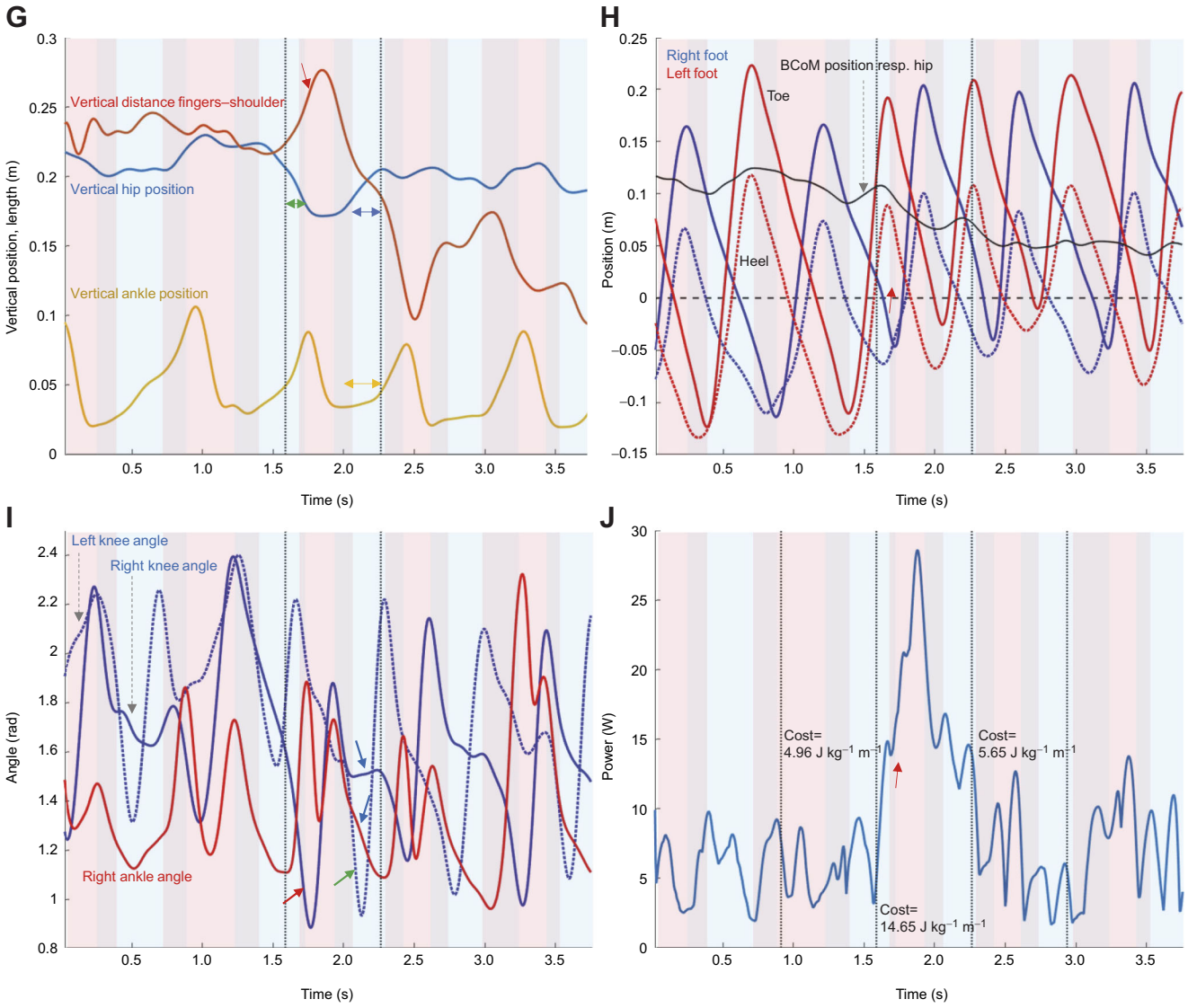

Fig. 3. Analysis of quadrupedal–bipedal transition 'on the fly' (worked example). In all panels: vertical dashed black lines indicate the start and end of the transition phase; blue and red shaded zones indicate the stance phases of the right (camera-side) and left (contralateral side) foot, respectively. (A) Determination of the transition period. The vertical velocity profile of the BCoM (red) bounds the transition phase (zero-crossing). The double-headed arrow refers to the period the BCoM/head–arms–trunk (HAT) CoM still rises despite the angular momenta (C) being close to zero (for details, see Results). (B) Forward displacement of the BCoM (dashed black curve) and its linear regression (blue curve; for details, see Results). (C) Total angular moment of the body and HAT (H_{HAT}). The red arrow indicates that H_{HAT} is close to zero in the time period spanned by the double-headed arrow in A. The blue arrow thus shows that, in this time span, the total body momentum is entirely captured in the moving hindlimbs (for details, see Results). (D) Angular position of the trunk. The double-headed arrow spans the same period as in A, during which no trunk rotation happens (linked to G; for details, see Results). (E) Moment of the total (blue curve), vertical (dashed green curve) and horizontal (dashed red curve) GRF about the BCoM. From the timing and direction of the oscillations, it is obvious that the total moment (blue curve; equal to the rate of change of the total angular momentum in C) is entirely determined by the vertical GRF component (green curve; for details, see Results). (F) Moment of the total GRF (blue curve) and PoA with respect of the BCoM (dashed green curve). Again, the timing and direction of the oscillations coincide indicating that the (rate of) change of the total angular momentum is primarily determined by PoA shifts (for details, see Results). (G) Vertical hip (blue curve) and ankle (ochre curve) displacement and vertical distance between shoulder and fingers tips (red curve). The double-headed blue arrow is as in D and A. During this time span, the hip moves up thus representing the rise of the BCoM and HAT CoM (A). The time period spanned by the double-headed green arrow coincides with downwards acceleration of the hip (hind parts) and can thus represent an early forwards shift of the PoA (arrow in F). The red arrow points at the instant the front limbs no longer contact the ground (no further potential contribution by arm pushing). The time period spanned by the double-headed ochre arrow indicates the height gain of the ankle as a result of tarso-metatarsal dorsiflexion. As the knee is hardly extending during this time span (blue arrow in I), this mechanism assists the above-mentioned hip rise (for details, see Results). (H) Relative fore–aft positioning of the feet and the BCoM with respect to the hip's (horizontal) position. The toe/heel contacts the ground whenever the according profile moves backwards with respect to the hip (i.e. decreasing relative position). In this way, stance periods are determined. The BCoM (black curve) moves backward with respect to the hip during most of the transition phase (except for the period spanned by the blue double-headed arrow in D and A) as a result of the upwards HAT (trunk) rotation (for details, see Results). (I) Knee (blue curve) and ankle (red curve) angles. The red arrow indicates the continued deep stance knee flexion when the transition is initiated. A similar deep knee flexion is present during the next contralateral stance (green arrow). During the subsequent stance of the limb that initiates the transition, the knee angle remains nearly constant (blue arrow at knee profile), whereas the ankle joint of the same limb decreases (blue arrow at ankle profile). This implies the forward rotation of the fixed hip–knee–ankle triangle about the ankle (for details, see Results). (J) Instantaneous metabolic power (conservative estimate: no transfer or elastic recovery) and metabolic costs for the transition period and a quadrupedal and bipedal period of identical duration as indicated by the additional vertical black dashed lines (for details, see Results).

into account. The used efficiency values are assumed to include the costs of force production while doing work. Clearly, isometric force production by muscles also comes with metabolic energy consumption. This is not included in the present estimate. The use of more elaborate cost functions (e.g. Alexander, 1997) is beyond the goal and scope of this paper.

Statistical analysis

Given the protocol previously described, the data are heterogeneous concerning the amount of steps that could be collected before and after the transition. Hence, exact non-parametric permutation tests for paired samples are applied to test for differences between (1) the quadrupedal walking gait and the subsequent transition period as delineated (see above), and (2) the transition and the subsequent bipedal walking gait.

Specifically, the variations in the touchdown position of the feet relative to the BCoM and hip were tested. Also, the step durations (i.e. the time between consecutive contralateral foot touchdowns) throughout the quadrupedal to bipedal transition were compared. The statistical tests were applied on dimensionless values because the present sample includes individuals of different size. The touchdown position of the foot relative to the BCoM and the hip was normalized by dividing its value by the shank length as measured directly on the respective individual (e.g. Aerts et al., 2000; Druelle et al., 2022b). The step duration was made dimensionless by dividing its value by the square root of the ratio of shank length over the gravitational acceleration (see Hof, 1996).

The dimensionless forward velocity and the cost of transport were compared between quadrupedal walking, the subsequent delineated transition and the subsequent bipedal walking. For this purpose, we used quadrupedal and bipedal bouts that were equivalent in length to the duration of the delineated transition. Only when sufficient walking steps were available before and/or after the transition could the comparison be made. As such, a subsample of 10 'quadrupedal walking to transition' and 8 'transition to bipedal walking' sequences could be retained in these comparisons. By comparing J kg^{-1} m^{-1}, effects of size and speed are taken into account for the cost of transport.

The contribution of the moment of the vertical and horizontal GRFs to $\dot{H}_{body}$ during the transition was tested using a congruity index, calculated as follows:

$$\text{Congruity index}_{GRF_y} = \frac{\sum_1^{n-1}[(M_{GRF_{y,n+1}} - M_{GRF_{y,n}})(\dot{H}_{body_{n+1}} - \dot{H}_{body_n}) > 0]}{n-1}, \quad (6)$$

where M_{GRF_y} is the moment of the vertical GRF and n is the number of data point in the transition time interval considered. The contribution moment of the horizontal GRF (Congruity $index_{GRF_x}$) was calculated in a similar way.

The statistics were conducted using the software for Exact non-parametric inference StatXact 3.1 (Cytel, Inc., Cambridge, MA, USA). The significance level was set at $P<0.05$ for all tests. The Bonferroni correction lowering the alpha level was applied when multiple comparisons were made between all the components of the transition (i.e. quadrupedal versus transition, quadrupedal versus bipedal, transition versus bipedal); this correction corresponds to 3 trials and is indicated with P'. In the following sections, the average values are given with their average absolute deviation (i.e. mean ±average deviation).

RESULTS AND DISCUSSION

Detailed description of the mechanics of the worked quadrupedal–bipedal transition example

This description is based on a transition bout performed by a juvenile (Fleur, see Table 1; body mass 2.85 kg, hip height in bipedal posture ∼0.2 m on the day of recording; see Movie 1). This individual and sequence were selected because the field of view and the size of the specimen enabled us to analyse 13 sequential steps at once (5 preceding quadrupedal, 2 pure transitional and 6 successive bipedal steps). The result of the entire procedure as described in Materials and Methods is represented in Movie 1 (animated stick figure, with the BCoM, GRF and PoA added). The orientation and position of the GRF regarding the BCoM being overall consistent with what can be predicted from basic mechanical principles proves the general reliability of the procedure. This becomes especially evident when considering the PoA (relying entirely on the magnitude and orientation of the calculated GRF and on the calculated BCoM position) during the bipedal walking phase: the position of the calculated PoA is always and meaningfully situated within the (fore–aft) boundary of the foot in stance (see Movies 1 and 2).

Fig. 3A illustrates how the transition *sensu stricto* is determined based on the vertical movements of the BCoM. Its displacement (blue solid curve) is in amplitude and profile largely similar to that of the HAT CoM (blue dashed curve) indicating that the HAT movements (rotation) dominate the transition. The start and end timing of the transition phase (dashed vertical lines) are given by the instants of the according zero-crossings of the vertical velocity of the BCoM (red curve). Pale blue and red regions in this graph (and in all other panels of Fig. 3) accord with the stance phase of the foot (right) at the camera-side and the contralateral (left) foot, respectively. Darker regions are the double stance periods.

Fig. 3B represents the forward displacement of the BCoM (black dashed curve) and its linear regression against time (blue curve). Clearly, the transition event itself does not affect the instantaneous walking speed (of 0.45 m s^{-1}) and based on the position–time profile alone, the event cannot be detected. This is a real on the fly transition at steady walking speed (R^2=0.99; see Materials and Methods).

The total angular momentum of the body (H_{body}) and the fraction taken by the HAT (H_{HAT}) throughout the walking sequence are illustrated in Fig. 3C. Clearly, H_{body} is to a great extent determined by the rotational movements of the HAT (also in the quadrupedal mode; the few bipedal steps are more irregular, which is expected because of the lower stability and the fact that the animal comes to a standstill at about time t=4 s). The difference between the body and HAT curves is the amount of rotation captured in the hindlimb oscillations, which is, overall (and logically), not very different for quadrupedal, transition and bipedal steps. As such, the (changes of) H_{HAT} in the transition phase largely represents the efforts spent in what distinguishes that phase from pure quadrupedal and bipedal walking: the upwards rotation of the HAT. During quadrupedal walking, H_{body} nicely oscillates about zero as dictated by basic mechanical principles (see the theoretical framework).

The quadrupedal–bipedal transition seems to be initiated at the instant H_{body} and H_{HAT} reach their maxima during the normal oscillations of quadrupedal striding (first dashed vertical line). Instead of dropping again, the momentum stays high/continues to increase for H_{body} and H_{HAT}, respectively. This happens prior to the next (left) foot placement. Apparently, (a) mechanism(s) other than 'foot repositioning' (see the theoretical framework), such as 'drop of the hind parts' or some 'upwards trust generation' from the arms, is

in play early in the transition. However, together with the succeeding left foot touchdown (onset of the red-shaded time interval, about 13% in the transition phase), H_{body} rises sharply, suggestive of the importance of 'foot repositioning' for the transition strategy (see theoretical framework). During the second half of the same left stance, H_{body} (and H_{HAT}) drop to zero, and although the BCoM further moves upwards during the subsequent step (see the region spanned by the blue double-headed arrow in Fig. 3A), the positive H_{body} peak in this period is nearly entirely captured in the hindlimb rotations (red arrow in Fig. 3C; H_{HAT} remains very small). Apparently, major HAT reorientations (angular changes) are realized within one single step, and the further upwards movement of the BCoM during the second half of what is defined as the transition phase (see above and Materials and Methods) derives primarily from the upwards vertical displacement of the hip during the second 'transition step' (region spanned by blue double-headed arrow in Fig. 3G), not from trunk rotation (see Fig. 3D, region spanned by blue double-headed arrow).

Whenever the H_{body} curve rises, the derivative ($\dot{H}_{body}$) is >0, meaning that the GRFs exert a counterclockwise moment (even when the momentum itself is still negative). Otherwise, when $\dot{H}_{body}$ <0, the opposite is true. Fig. 3E presents $\dot{H}_{body}$ (blue) together with its components as derived from the horizontal (red) and vertical (green) GRFs. The message from this graph is clear and straightforward: changes of H_{body} (blue peaks) accord (in timing and direction) nearly exclusively with the moments generated by the vertical GRFs (green peaks). In other words, fore–aft accelerations seem to play hardly any role of importance in the on the fly quadrupedal–bipedal transition. Moreover, as vertical GRFs always point upwards, the fluctuations about zero of $\dot{H}_{body}$ appear nearly exclusively regulated by shifts of the PoA, not by changes of the magnitude or orientation of the GRFs. This is confirmed by plotting the PoA (×10; green curve) together with $\dot{H}_{body}$ (blue curve; Fig. 3F). Both graphs fluctuate nearly perfectly in phase.

As mentioned in the theoretical framework, however, time fluctuations of the moments of the GRFs (in terms of varying magnitudes, orientations and positions) only reflect the underlying strategy used to carry out the quadrupedal–bipedal transition on the fly. To unravel this, we must therefore now evaluate the potential roles of 'drop of the hind parts', 'arm push' and 'foot repositioning'.

During approximately the first 13% of what is defined as the transition phase, the diagonal limb pair (right hindlimb, left forelimb) is in contact with the ground, with the foot far behind the position of the BCoM (even behind the hip; see Fig. 3H). Therefore, either 'drop of the hind parts' and/or 'arm push' must be in play during this initial phase of the transition. As argued in the theoretical framework, (downwards accelerating) hip drop and arm push can cause (all or not together) a forward shift of the PoA. Fig. 3G shows that both mechanisms might be in play initially in the transition. The hip (blue curve) is accelerating downwards (region spanned by the green double-headed arrow), while the vertical distance between the fingers and shoulder of the left arm increases (red curve; red arrow indicates end of ground contact). This is further confirmed by the forward displacement of the PoA (in front of the BCoM) initially in the transition (red arrow in Fig. 3F), but notice that the observed arm extension can equally well be passive (i.e. no real upwards pushing) because of trunk rotation at the hip.

In the theoretical framework, it was also mentioned that lowering the hips as such can cause a re-orientation of the trunk (HAT) provided the shoulders keep the same height. However, the (maximal) contribution of such reconfiguration is only a small fraction of the total trunk rotation as shown in Fig. 3D: based on geometry, at its deepest position, the hip drop can represent only 16% of the total rotation. Even during this initial phase (before the left foot touchdown), the trunk rotation almost triples what could be expected from the hip drop directly. In other words, it cannot be excluded that arm extension (see initial rise of the red curve in Fig. 3G) does contribute to some extent actively to the very initial phase of the quadrupedal–bipedal transition.

For what follows it is important to focus briefly on what causes the oscillation of the hip height during the transition as illustrated in Fig. 3G (blue curve between the dashed vertical lines). Fig. 3H shows the foot positioning with regard to the hip (and the BCoM). The blue curves (solid, toe; dashed, heel) represent the position of the right foot regarding the hip (horizontal dashed line at zero position), the red curves represent the left foot. Declining curves correspond to the ground contact phase, rising curves represent the swing phase. The black solid line is the position of the BCoM with respect to the hip. It is obvious that lowering of the hip early in the transition is not the result of a pronounced more forward touchdown position of the feet in the transition steps. The more likely explanation for the vertical hip oscillation is the knee kinematics. Knee flexion continues during the stance of the right foot when transition is initiated (red arrow in Fig. 3I; solid blue curve: right knee angle, dashed blue curve: left knee angle), as well as during the subsequent stance of the left foot (green arrow). As a result, the hip drops during the first part of the transition. The subsequent rising of the hip is, at first glance, somewhat puzzling. There is no obvious limb extension going on during this phase. During the single stance phase of the next right step (coincident with the upwards movement of the hip), the knee angle remains almost constant and the ankle angle decreases (blue arrows in Fig. 3I). However, as a consequence of the 'constant knee angle' in this phase, the hip–knee–ankle configuration forms a quasi-fixed triangle. As the ankle is in front of the hip, retraction of the limb (i.e. the fixed triangle rotates about the 'ankle point') must go along with the upwards displacement of the hip. Moreover, this rotation forces the tarso-metatarsal joint into dorsiflexion which will contribute to the hip rise, too (as illustrated by the small vertical height gain of the ankle in Fig. 3G; ochre curve, region spanned by double-headed arrow). The re-gain in hip height obtained in this way corresponds remarkably well to what can be observed in Fig. 3G. We will return to the knee behaviour later.

However, at least from the moment the left hand loses ground contact onwards, 'foot repositioning' is the only remaining mechanism that can contribute to the transition, as the hip is at that moment close to its deepest position (and is definitely not accelerating downwards anymore). Despite the fact that the foot positioning at touchdown with regard to the hip (i.e. the suspension point of the swinging limb) remains fairly unchanged (Fig. 3H), the foot positioning with respect to the BCoM does change (Fig. 3H): in a sequence of three steps (left–right–left) during the transition, the foot positioning changes from oscillating nearly entirely behind the BCoM in the quadrupedal mode, to oscillating beneath the BCoM in the bipedal mode (Fig. 3H). This can happen because the BCoM moves backwards relative to the hip mainly as the result of the upwards rotation of the heavy HAT, but equally well because the hindlimbs become considerably less retracted with regard to the hip during the transition phase (as well as during the subsequent bipedal sequence; Fig. 3H). In other words: smaller steps are made at a higher frequency (remember, the overall walking speed is fairly constant; see Fig. 3B). This reduced limb retraction actually happens at the end of the quadrupedal hindlimb stance preceding the transition phase (and continuing during the first 13% of it). This strongly indicates that the reduced limb retraction is definitely part

Journal of Experimental Biology (2023) 226, jeb244792. doi:10.1242/jeb.244792

of the transition strategy and is not the consequence of anatomical constraints at the level of the hip. Indeed, early in the transition phase, increase of the hip angle as a result of upwards HAT rotation is still very limited. Moreover, although maximal hip angles at the end of stance become clearly larger throughout the transition, these seem still to be smaller than what occasionally happens during bipedal walking.

All together and worded in a simplified way, the transition strategy applied in this example sequence could be summarized as: crouch the hind parts and sprint them underneath the rising BCoM. This does not mean, however, that the transition is made effortless. Fig. 3J represents the conservative estimation (no energy transfer between segments, no elastic recoveries) of the metabolic power (see Materials and Methods). Integrated over the transition phase and expressed per kg body mass and per unit distance covered, the energy spent in the transition (14.24 J kg^{-1} m^{-1}) roughly triples that spent during quadrupedal (4.62 J kg^{-1} m^{-1}) and bipedal (4.67 J kg^{-1} m^{-1}) walking. Given the magnitudes presented on the graph, it appears that the transition on the fly does not, however, require exceptional efforts. A gentle, playful jump starting from a crouched standstill position of only about 20 cm high is easy to imagine for the young individual executing the present example sequence. From basic principles (change of kinetic energy during push off equals the work done by all external forces; efficiency of 0.25), the costs of such a gentle playful jump can be estimated to be about fivefold the costs for the transition, while the power requirements exceed those for the transition by even more.

Still, the energy input for the transition must be delivered by muscles working concentrically (positive work). We argue that this must come primarily from the hip extensors. Indeed, Fig. 3I suggests that early in the transition, knee extensors work eccentrically (negative work) throughout stance (preventing collapse of the continuously flexing knee). The upwards rotation of the heavy HAT shown in Fig. 3D must be powered primarily by hip extensors. At the end of the transition, the BCoM is still moving further upwards, yet without trunk rotation. The knee is delivering no work (as the knee angle hardly changes). We argue that the vertical translation of the HAT is caused by limb retraction and thus hip extensor torque must be considered again as the primary motor of this part of the transition phase.

Finally, it is worth mentioning that foot repositioning has important consequences. Although the BCoM moves towards the hip, the latter always stays behind the BCoM. This inevitably implies a bent-hip–bent-knee bipedal posture in order to ensure that the support bases of the feet oscillate beneath the BCoM as needed for stable bipedal walking. As bipedal walking in bent-hip–bent-knee walking primates remains hip driven (see above and Druelle et al., 2022a), but also because body weight and inertial forces during walking tend to collapse the bent hip and knee joints, bipedal walking in non-human primates probably remains a strenuous locomotor mode if continued for long periods (for an elaborate discussion on this, see Druelle et al., 2022a).

Testing the hypotheses about the quadrupedal–bipedal transition strategy across the full sample

Hypothesis 1: the transition from quadrupedal to bipedal locomotion is effectively performed on the fly

From Fig. 3B, it is obvious this holds true for the transition of the worked transition example. The forward velocity is constant over the preceding five quadrupedal steps, the two pure transitional steps and the successive six bipedal steps (linear regression R^2=0.99 in Fig. 3B). Although all transitions are executed as a single smooth and continuous movement sequence (see stick figure animations in Movie 2; R^2 values of linear regression of the forward displacement throughout the transition are always >0.94), the high constancy of the forward velocity is not entirely confirmed across the full sample. Making use of the dimensionless forward velocity of the hip as the reference for locomotor speed, it appears that the dimensionless forward velocity during the transition phase is statistically indifferent from the dimensionless speed during the preceding quadrupedal phase (paired permutation test=−0.89, P=0.40; Fig. 4). However, the subsequent bipedal walking is significantly slower (paired permutation test=2.30, P=0.008; Fig. 4). Dimensionless locomotor speed as measured from the BCoM does not show a significant result between the quadrupedal phase and the transition, nor between the transition and the subsequent bipedal walking (paired permutation test=1.746, P=0.07, and paired permutation test=1.65, P=0.11, respectively; Fig. 4). During the transition phase, dimensionless BCoM speed is significantly lower than the hip speed (paired permutation test=−3.76, P=0.0001), because relative to the hip the BCoM moves backwards as a result of the upwards and backwards rotation of the heavy HAT. All in all, across the full sample, baboons slow down a bit when transitioning from quadrupedal to bipedal walking on the fly. Most probably, this slight deceleration is imposed by the experimental setup: the baboons approached the end of the technical platform and were thus forced to slow down and eventually stop their forward movement (see Materials and Methods). Regardless, an interruption of the

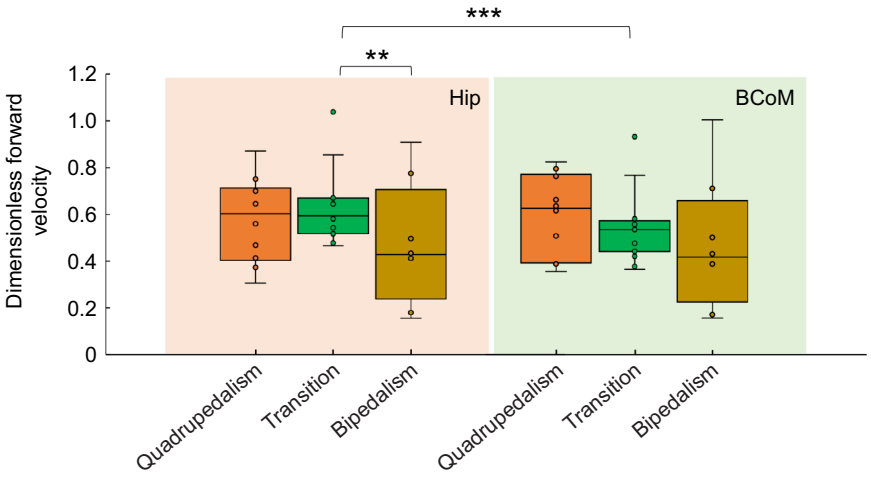

Fig. 4. Box plots of the dimensionless forward velocity throughout the transition, estimated from the hip joint and the BCoM. Boxes show 25th and 75th percentiles with median; whiskers indicate minimal and maximal values which remain inside the 1.5x interquartile range (IQR); higher and lower values are outliers. **P<0.01, ***P<0.0001.

Journal of Experimental Biology (2023) 226, jeb244792. doi:10.1242/jeb.244792

forward progression to make the quadrupedal–bipedal transition was never observed (see Movie 2). Neither was there a forward acceleration to make the transition possible (see theoretical framework; see below).

Because of the differences in quadrupedal approach speed, cycling frequency and size of the individuals, the observed duration of the transition phases was variable and ranged from 0.3 to 0.88 s, with an average of 0.61 s. In practice, this implies that the transition is commonly performed within two steps (11/15), but one transition was performed within three steps and three transitions within one step.

Hypothesis 2: all individuals use a similar strategy

Based on the detailed analysis of the worked example, the strategy of this transition basically boils down to: crouch the hind parts and sprint them underneath the rising BCoM. Foot positioning shifts from behind to 'in front of' the BCoM. Furthermore, the same analysis proves that this 'sprinting' does not imply a sudden and momentary forward acceleration of the BCoM, but accompanies an increased frequency of smaller stepping cycles. This strategy appears pretty consistent over the full sample.

Crouching the hind parts (at the start of the transition)

For this, we tested whether hip height decreases between the initiation of the transition and at 13% of the transition (see the description of the worked example). There was a significant decrease in hip height (after size correction, from 1.77±0.18 to 1.73 ±0.20) between the start of the transition and at 13% of the transition (paired permutation test=2.19, P=0.02; Fig. 5).

Sprint the hind parts underneath the rising BCoM by positioning the feet further forward at higher stepping frequencies

The dimensionless step duration (1/step frequency) decreased significantly during the transition, i.e. the amount of time between the last foot touchdown before the transition and the next foot touchdown in the transition decreased significantly (Fig. 6A), but there was no other difference in the interlimb stepping frequency (step 1 versus step 2: 3.38±0.52 versus 3.51±0.60, paired permutation test=−1.29, P=0.22; step 2 versus step 3: 3.51±0.60 versus 3.08±0.85, paired permutation test=2.34, P=0.01; step 3 versus step 4: 3.08±0.85 versus 2.67±0.53, paired permutation test=1.48, P=0.14; step 4 versus step 5: 2.67±0.53 versus 2.94 ±0.35, paired permutation test=−1.45, P=0.19; step 5 versus step 6: 2.94±0.35 versus 3.28±0.66, paired permutation test=−0.74, P=0.52).

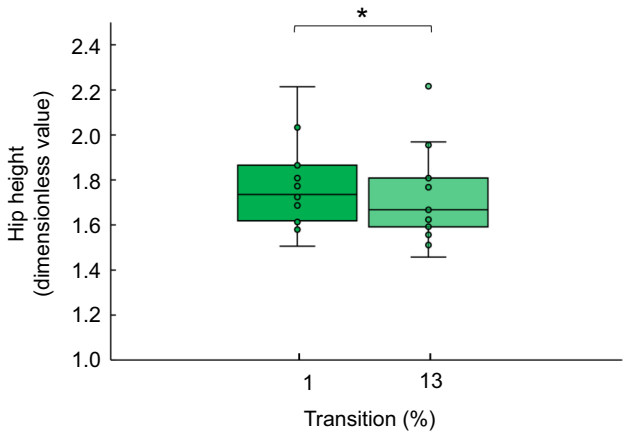

Fig. 5. Box plots of the dimensionless hip height at the start of the transition and at 13% of the transition period. Boxes show 25th and 75th percentiles with median; whiskers indicate minimal and maximal values which remain inside the 1.5x interquartile range (IQR); higher and lower values are outliers. *P<0.05.

When considering consecutive touchdown positions of the contralateral legs with respect to the hip, no significant differences could be found during quadrupedal walking, during the transition and during bipedal walking (1.59±0.18 versus 1.70 ±0.18, paired permutation test=−1.56, P=0.13; 1.86±0.21 versus 1.71±0.24, paired permutation test=1.53, P=0.13; 1.50±0.26 versus 1.52±0.14 paired permutation test=−0.16, P=0.91, respectively), as well as when the quadrupedal walking was compared with the transition (1.70±0.18 versus 1.86±0.21, paired permutation test=−1.81, P=0.07) and when the transition was compared with bipedal walking (1.71±0.24 versus 1.50±0.26, paired permutation test=1.55, P=0.09; Fig. 6Bi).

When considering each leg separately (i.e. focusing on consecutive footfalls of the same leg, right and left separately), there was a trend toward a significant difference (very close to the significance threshold), in the touchdown position with respect to the hip for the leg of which the foot touches down at the onset of the delineated transition (i.e. leg1) when quadrupedal walking and the transition are compared; no differences were found for the other leg (leg2) (leg1: 1.59±0.18 versus 1.86±0.21, paired permutation test=−1.963, P=0.05; leg2: 1.70±0.18 versus 1.71±0.24, paired permutation test=−0.018, P=0.98; Fig. 6Bi). This means that the first leg that touches down at the onset of the transition tends to be positioned more in front of the hip, compared with its position during the previous quadrupedal behaviour.

Concerning consecutive touchdown positions of the contralateral legs with respect to the BCoM, no significant differences could be found during quadrupedal walking (0.72±0.20 versus 0.78±0.20, paired permutation test=−1.28, P=0.21), during the transition (1.07 ±0.26 versus 1.15±0.26, paired permutation test=−0.84, P=0.42) and bipedal walking (1.09±0.31 versus 1.07±0.25, paired permutation test=−0.04, P=0.91). There was, however, a significant difference in touchdown position relative to the BCoM between the contralateral legs when quadrupedal walking and the transition were compared, but not when the transition was compared with bipedal walking (leg1−leg2: 0.78±0.20 versus 1.07±0.26, paired permutation test=−2.80, P=0.002; 1.15±0.26 versus 1.09 ±0.31, paired permutation test=1.11, P=0.41, respectively; Fig. 6Bii).

When comparing consecutive footfalls of the same leg, there was a significant difference of the touchdown position relative to the BCoM for both legs when quadrupedal walking and the transition were compared (leg1: 0.72±0.20 versus 1.07±0.26, paired permutation test=−2.16, P=0.02; leg2: 0.78±0.20 versus 1.15 ±0.26, paired permutation test=−2.87, P=0.0007). The transition has a significant impact on the foot placement relative to the BCoM. Both legs that touch down during the transition are positioned significantly more in front of the BCoM, compared with their respective position during the previous quadrupedal behaviour (Fig. 6Bii).

Sudden and momentary forward acceleration of the BCoM plays no role in the transition

This is obvious from the evaluation of hypothesis 1. If there is a significant difference in the average forward speed of the subsequent sections throughout the transition, it is a decrease in speed (i.e. deceleration; see Fig. 4). Moreover, if forward acceleration was in play, this should be reflected in the moment

Journal of Experimental Biology (2023) 226, jeb244792. doi:10.1242/jeb.244792

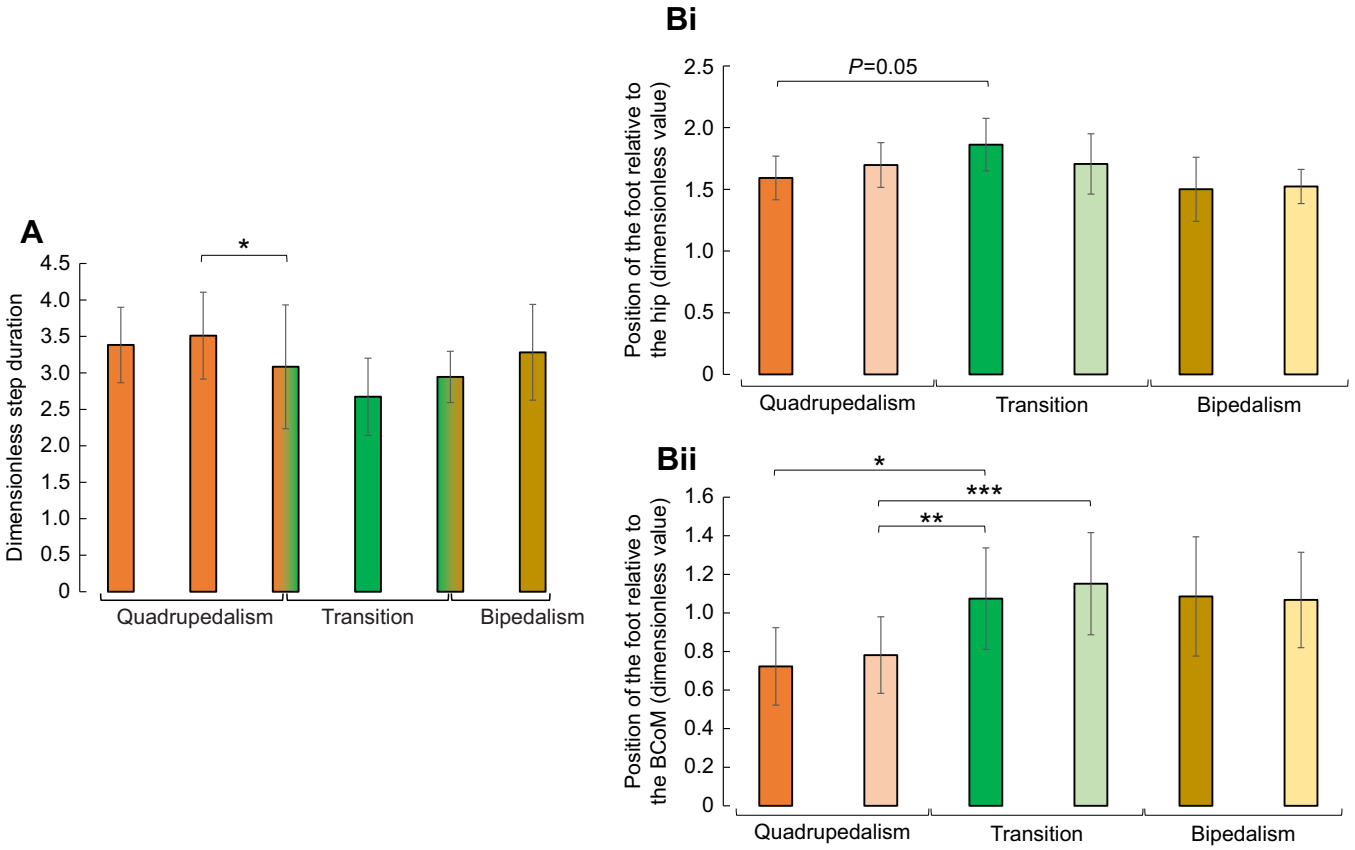

Fig. 6. Spatio-temporal gait features throughout transition. (A) Dimensionless step duration of the hindlimbs throughout the quadrupedal to bipedal transition (orange: quadrupedal, green: transition; ochre: bipedal). (B) Touchdown positions of the foot relative to (i) the hip and (ii) the BCoM after size correction (orange: quadrupedal; green: transition; ochre: bipedal; dark-coloured: leg1; light-coloured: leg2). *P<0.05, **P<0.01, ***P<0.0001.

generated by the horizontal GRF about the BCoM (see theoretical framework and detailed description of the worked example). Fig. 7 shows the congruity index for the moment of the vertical GRF and the moment of the horizontal GRF with the rate of change of the total angular momentum of the body ($\dot{H}_{body}$). There was a significant difference in the congruity index of the two moments (66±10% versus 46±11%, paired permutation test=2.75, P=0.001).

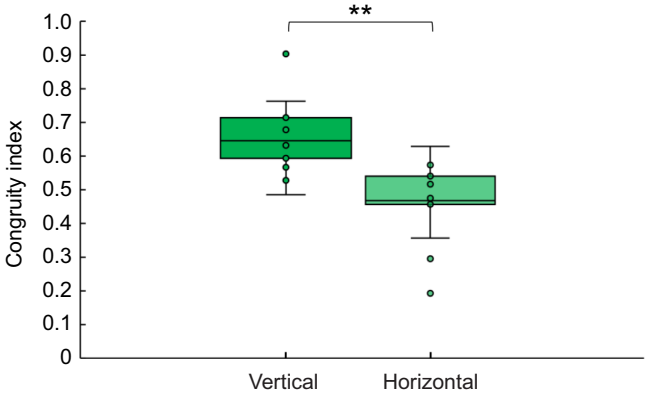

Fig. 7. Box plots of the congruity indices of the moments of the planar components of the GRF with the total angular momentum of the body ($\dot{H}_{body}$) during the transition. Boxes show 25th and 75th percentiles with median; whiskers indicate minimal and maximal values which remain inside the 1.5x interquartile range (IQR); higher and lower values are outliers. **P<0.01.

The moment of the vertical GRF was more congruent with $\dot{H}_{body}$ than was the horizontal moment.

From a motor control perspective, this dynamic transition strategy, primarily involving a change in stride frequency and foot positioning, reflects adjustment of the motor coordination of the individual limb joints (Maes and Abourachid, 2013; Mori et al., 2006). Such a change in limb kinematics also affects the dynamic stability (see Fig. 3C) for reaching a new stable (bipedal) state. Hip extensor torques probably play a significant role in the initiation and control of the transition (see detailed description of the worked example). However, it does not imply any break in the coordination pattern controlled by the nervous system. The on the fly quadrupedal to bipedal transition observed in baboons is therefore a good example of the shared quadrupedal and bipedal coordination in a non-adapted biped (see also Druelle et al., 2017a).

Hypothesis 3: the transition implies limited extra costs and efforts compared with normal quadrupedal and bipedal locomotion

There was no statistical difference in the metabolic cost between quadrupedal and bipedal walking before and after the transition (quadrupedalism: 8.58±3.23 J kg^{-1} m^{-1} versus bipedalism: 6.45 ±2.78 J kg^{-1} m^{-1}; paired permutation test=0.72, P'=0.59). There was a significant difference in the metabolic cost between quadrupedal walking and the transition and between the transition and bipedal walking (transition: 15.26±3.75 J kg^{-1} m^{-1}; paired permutation test=−2.29, P'=0.02; permutation test=2.653, P'=0.0234, respectively; Fig. 8). On average, the costs for the transition *sensu stricto* of a quadrupedal–bipedal on the fly

Journal of Experimental Biology (2023) 226, jeb244792. doi:10.1242/jeb.244792

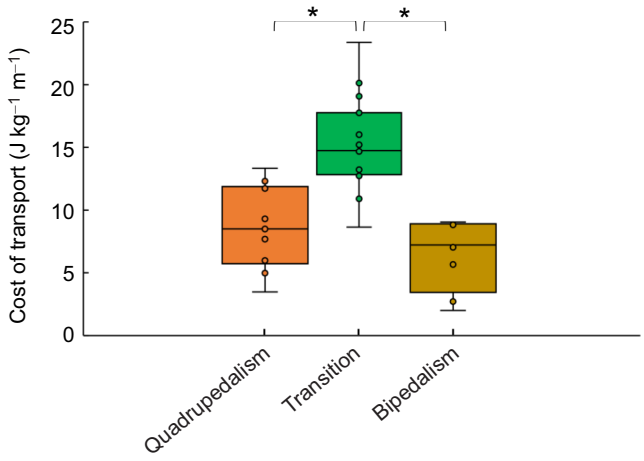

Fig. 8. Box plots of the cost of transport throughout the transition. Boxes show 25th and 75th percentiles with median; whiskers indicate minimal and maximal values which remain inside the 1.5x interquartile range (IQR); higher and lower values are outliers. *P<0.05.

transition approximately doubled, compared with the costs for the preceding quadrupedal or following bipedal walking.

These estimates of the extra costs are 'maximal' in a sense that no energy transfer or recuperation is taken into account. As already argued when discussing the worked transition example, we believe that the energetic costs to perform quadrupedal–bipedal transitions on the fly are negligible when considered in the context of the normal locomotor repertoire of baboons, including gait initiations (involving abrupt accelerations), sit to stand transitions, climbing, manoeuvring, high speed gaits, etc. (see 'Evolutionary perspectives', below).

Comparative aspects

To our knowledge, only one other study in primates deal with the dynamic quadrupedal–bipedal transition. It was observed that *Macaca fuscata* keeps a steady forward walking speed during the quadrupedal to bipedal transition (Nakajima et al., 2001). In addition, the researchers showed that gaze was maintained (on the food reward in the context of their setup on a treadmill) by continuous changes in head orientation. Although we did not focus on gaze, we can assume that during the transition observed in baboons, the animals were targeting a point in the mirror (see Materials and Methods). Nakajima et al. (2001) defined the beginning of the transition at touchdown of the hindlimb that provokes an upward excursion of the angle of the weight-bearing hip joint. This leads to the freeing of the forelimbs from the constraints of supporting the body and results in a bipedal walking gait. Although the delimitation of the transition is different from our study, the qualitative description provided by Nakajima et al. (2001) allowed us to suggest that macaques may use a similar strategy to baboons by, at least, repositioning one hindlimb at touchdown, thus provoking the required additional positive moment about the BCoM. Strategies using variations in phase shift and rhythm have also been proposed, in legged robots performing a quadrupedal to bipedal transition (Aoi et al., 2012). However, as pointed out by Aoi et al. (2012), the general performance of the robots remains generally low compared with the performance observed in animals. For instance, baboons are complex organisms and use a dynamic strategy integrating stride length and frequency to make the transition on the fly. A relevant observation from our study lies in the foot re-positioning relative to the BCoM, the increased stride frequency and the implication of the hip extensor torques which play significant roles in the initiation and control of this transition. Some of these aspects have been implemented in the transition strategy of robots, but in a very different way from the strategy observed in baboons. Therefore, we believe that the way we describe it in this study can inspire the creation of new control strategies in robots, possibly towards more flexible abilities.

Evolutionary perspectives

In their daily activities, primates regularly change their posture by completely reorienting their body segments. For instance, many transitions happen in the trees (e.g. Thorpe and Crompton, 2006), which are inherent to coping with the complexity of the arboreal environment. For decades, positional repertoires (locomotor and postural modes) have been quantified by researchers to capture and frame the complexity of the locomotion of primates (e.g. Hunt et al., 1996; Prost, 1965). Although this is a relevant magnifying glass providing a good theoretical framework for many (eco-functional) purposes (Cant, 1992; Hunt, 2016), lots of these modes are commonly irregularly performed and do not follow patterned activities (Biewener and Daley, 2007; Fleagle et al., 1981). This of course represents a challenge for further analyses and descriptions, but it also results in an emerging framework including transitions between locomotor modes. Transitions must be effectively performed in many activity contexts (e.g. food carrying, display, investigation, social greetings, etc.) as well as to negotiate arboreal environments (e.g. Bailey et al., 2020; Dunham, 2015; Isler and Grüter, 2006; Myatt et al., 2011; Myatt and Thorpe, 2011; Thorpe and Crompton, 2006; Zhu et al., 2015). While body plans can be adapted to specific locomotor modes and capacities (e.g. Preuschoft, 1989; Preuschoft, 2004; Preuschoft and Günther, 1994), the capability of (arboreal) primates to transition between locomotor modes might also be under strong selective pressures.

From an evolutionary perspective, the onset of new specialized locomotor modes, such as brachiation, bipedalism, inverted quadrupedal walking, arm swinging, etc., requires ancestors having predisposed morphologies and locomotor capabilities (Fleagle et al., 1981; Granatosky and Schmitt, 2019; Rose, 1991), in addition to the capacity to operate instantaneous locomotor transitions during their daily activities. Upright gaits obviously introduce loading constraints for the hindlimbs and increased demands in balance (Higurashi et al., 2019). However, bipedalism and quadrupedalism may share the same basic neuromotor mechanisms, at least in non-adapted bipeds (see above; e.g. Aerts et al., 2000; Frigon, 2017; Nakajima et al., 2004; Zehr et al., 2009), which makes the relationship between these two locomotor modes even more subtle than first expected. Furthermore, bipedal walking in chimpanzees has been shown to not be significantly more costly than quadrupedalism (Kimura and Yaguramaki, 2009; Pontzer et al., 2014; Sockol et al., 2007). Our study seems to confirm this finding for locomotor costs in quadrupedal and bipedal baboons. Sockol et al. (2007) suggested that only a few variations in morphology, such as hip extension and leg length, would have substantially improved bipedal walking efficiency above the level of quadrupedal walking efficiency in a *Pan*-like common ancestor. This hypothesis, when coupled to the results of Young et al. (2010) about the low level of interlimb integration in hominoids, and the results of Kozma et al. (2018) about hip extension in chimpanzees, allow us to suggest that, in early hominins, whose evolution of relatively longer legs was thus facilitated and hip extension made possible, an economical bipedal walking gait was already present at

this early stage of evolution (Kozma et al., 2018). As a result, considering an early hominin with increased bipedal walking capacities is possible (Kozma et al., 2018; Pontzer et al., 2014; Thompson et al., 2015; White et al., 2015). In addition, and in the light of the present results, the idea of an ancestor of hominins (in Miocene apes), capable of transitioning from one mode to another (for instance from quadrupedal to bipedal) using kinematic and dynamic strategies and avoiding a significant increase in energetic inputs is possible. Early hominins and their ancestors might thus have used, amongst others, habitual bipedalism in addition to a certain form of habitual quadrupedalism, including the smooth transitions between both in their locomotor repertoire. This does not exclude, however, that other locomotor modes, such as suspensory locomotion or climbing, were used as well within a large locomotor repertoire as observed in extant apes.

Conclusion

Baboons are able to transition from quadrupedal to bipedal walking in a smooth and non-erratic way, without any significant interruption in their forward movement (i.e. making a transition on the fly). The motor strategy to do so boils down to crouching the hind parts and sprinting them underneath the rising BCoM. Instantaneous forward accelerations play no role. Given the short duration of the transition as such (<1 s), the costs linked to these dynamical (on the fly) quadrupedal–bipedal transitions are estimated to be small and negligible when considered in the context of the normal locomotor repertoire of baboons. As a quadrupedal primate, being able to transition on the fly from quadrupedal to bipedal locomotion in a smooth, rapid and apparently rather effortless way may have been important when considering the ecological/evolutionary context.

Acknowledgements

We are very grateful to Guy Dubreuil, the director of the Primatology Station of the CNRS at the time the data were collected, who provided access to the animals and to the facilities of the station. We are very grateful to Christophe Arnoult, the current director of the Primatology Station of the CNRS, for his support, as well as to Romain Lacoste. We thank Guillaume Daver and Zohreh Anvari for their help in recording the video sequences of quadrupedal and bipedal walking in baboons.

Competing interests

The authors declare no competing or financial interests.

Author contributions

Conceptualization: P.A.; Methodology: P.A., F.D.; Software: P.A., J.G.; Formal analysis: P.A., J.G., F.D.; Investigation: P.A., F.D.; Resources: G.B., K.D., F.D.; Writing - original draft: P.A., F.D.; Writing - review & editing: P.A., F.D., G.B., K.D.; Funding acquisition: P.A., G.B.

Funding

This research was supported by a grant from FWO-Flanders and the Research Council of the University of Antwerp to P.A. (K803019N and BOF/SABBAT - IDnr.: 40504, respectively). The Technical Platform has been initially funded by the CNRS-INEE. This project is also currently funded by Agence Nationale de la Recherche ANR-18-CE27-0010-01 (G. Berillon Dir.) and CNRS-INEE International Research Network IRN-GDRI0870.

Data availability

Morphometric data on the specimens are provided as supplementary material.

References

Aerts, P., Van Damme, R., Van Elsacker, L. and Duchene, V. (2000). Spatio-temporal gait characteristics of the hind-limb cycles during voluntary bipedal and quadrupedal walking in bonobos (*Pan paniscus*). *Am. J. Phys. Anthropol.* **111**, 503-517. doi:10.1002/(SICI)1096-8644(200004)111:4<503::AID-AJPA6>3.0.CO;2-J

Aerts, P., Van Damme, R., D'Août, K. and Van Hooydonck, B. (2003). Bipedalism in lizards: whole-body modelling reveals a possible spandrel. *Phil. Trans. R. Soc. B* **358**, 1525-1533. doi:10.1098/rstb.2003.1342

Alexander, R. M. (1997). Optimum muscle design for oscillatory movements. *J. Theor. Biol.* **184**, 253-259. doi:10.1006/jtbi.1996.0271

Alexander, R. M. (2003). *Principles of Animal Locomotion*. Princeton University Press.

Anvari, Z., Berillon, G., Asgari Khaneghah, A., Grimaud-Herve, D., Moulin, V. and Nicolas, G. (2014). Kinematics and spatiotemporal parameters of infant-carrying in olive baboons. *Am. J. Phys. Anthropol.* **155**, 392-404. doi:10.1002/ajpa.22576

Aoi, S., Egi, Y., Sugimoto, R., Yamashita, T., Fujiki, S. and Tsuchiya, K. (2012). Functional roles of phase resetting in the gait transition of a biped robot from quadrupedal to bipedal locomotion. *IEEE Trans. Robot.* **28**, 1244-1259. doi:10.1109/TRO.2012.2205489

Bailey, K. E., Winking, J. W., Carlson, D. L., Van Bang, T. and Long, H. T. (2020). Arm-swinging in the red-shanked douc (*Pygathrix nemaeus*): implications of body mass. *Int. J. Primatol.* **41**, 583-595. doi:10.1007/s10764-020-00163-6

Balter, J. E. and Zehr, E. P. (2007). Neural coupling between the arms and legs during rhythmic locomotor-like cycling movement. *J. Neurophysiol.* **97**, 1809-1818. doi:10.1152/jn.01038.2006

Berillon, G., Daver, G., D'Août, K., Nicolas, G., de la Villetanet, B., Multon, F., Digrandi, G. and Dubreuil, G. (2010). Bipedal versus Quadrupedal hind limb and foot kinematics in a captive sample of *Papio anubis*: setup and preliminary results. *Int. J. Primatol.* **31**, 159-180. doi:10.1007/s10764-010-9398-2

Biewener, A. A. and Daley, M. A. (2007). Unsteady locomotion: integrating muscle function with whole body dynamics and neuromuscular control. *J. Exp. Biol.* **210**, 2949-2960. doi:10.1242/jeb.005801

Blickhan, R., Andrada, E., Hirasaki, E. and Ogihara, N. (2021). Trunk and leg kinematics of grounded and aerial running in bipedal macaques. *J. Exp. Biol.* **224**, jeb225532. doi:10.1242/jeb.225532

Blickhan, R., Andrada, E., Hirasaki, E. and Ogihara, N. (2018). Global dynamics of bipedal macaques during grounded and aerial running. *J. Exp. Biol.* **221**, jeb178897. doi:10.1242/jeb.178897

Cant, J. G. H. (1992). Positional behavior and body size of arboreal primates: a theoretical framework for field studies and an illustration of its application. *Am. J. Phys. Anthropol.* **88**, 273-283. doi:10.1002/ajpa.1330880302

Carvalho, S., Biro, D., Cunha, E., Hockings, K., McGrew, W. C., Richmond, B. G. and Matsuzawa, T. (2012). Chimpanzee carrying behaviour and the origins of human bipedality. *Curr. Biol.* **22**, R180-R181. doi:10.1016/j.cub.2012.01.052

Crompton, R. H., Li, Y., Alexander, R. M., Wang, W. and Gunther, M. M. (1996). Segment inertial properties of primates: new techniques for laboratory and field studies of locomotion. *Am. J. Phys. Anthropol.* **99**, 547-570. doi:10.1002/(SICI)1096-8644(199604)99:4<547::AID-AJPA3>3.0.CO;2-R

Demes, B. (2011). Three-dimensional kinematics of capuchin monkey bipedalism. *Am. J. Phys. Anthropol.* **145**, 147-155. doi:10.1002/ajpa.21484

D'Août, K., Vereecke, E., Schoonaert, K., De Clercq, D., Van Elsacker, L. and Aerts, P. (2004). Locomotion in bonobos (Pan paniscus): differences and similarities between bipedal and quadrupedal terrestrial walking, and a comparison with other locomotor modes. *J. Anat.* **204**, 353-361. doi:10.1111/j.0021-8782.2004.00292.x

Dietz, V. (2002). Do human bipeds use quadrupedal coordination? *Trends Neurosci.* **25**, 462-467. doi:10.1016/S0166-2236(02)02229-4

Dietz, V., Fouad, K. and Bastiaanse, C. M. (2001). Neuronal coordination of arm and leg movements during human locomotion. *Eur. J. Neurosci.* **14**, 1906-1914. doi:10.1046/j.0953-816x.2001.01813.x

Druelle, F. and Berillon, G. (2014). Bipedalism in non-human primates: a comparative review of behavioural and experimental explorations on catarrhines. *BMSAP* **26**, 1-10. doi:10.1007/s13219-014-0105-2

Druelle, F., Aerts, P. and Berillon, G. (2016). Bipedality from locomotor autonomy to adulthood in captive olive baboon (Papio anubis): Cross-sectional follow-up and first insight into the impact of body mass distribution. *Am. J. Phys. Anthropol.* **159**, 73-84. doi:10.1002/ajpa.22837

Druelle, F., Aerts, P. and Berillon, G. (2017a). The origin of bipedality as the result of a developmental by-product: The case study of the olive baboon (*Papio anubis*). *J. Hum. Evol.* **113**, 155-161. doi:10.1016/j.jhevol.2017.07.010

Druelle, F., Aerts, P., D'Août, K., Moulin, V. and Berillon, G. (2017b). Segmental morphometrics of the olive baboon (*Papio anubis*): a longitudinal study from birth to adulthood. *J. Anat.* **230**, 805-819. doi:10.1111/joa.12602

Druelle, F., Abourachid, A., Vasilopoulou-Kampitsi, M. and Aerts, P. (2022a). Convergence of bipedal locomotion: why walk or run on only two legs. In *Convergent Evolution: Animal Form and Function* (ed. V. Bels and A. P. Russel): Springer.

Druelle, F., Özçelebi, J., Marchal, F. and Berillon, G. (2022b). Development of bipedal walking in olive baboons, *Papio anubis*: A kinematic analysis. *Am. J. Biol. Anthropol.* **177**, 719-734. doi:10.1002/ajpa.24454

Dunham, N. T. (2015). Ontogeny of positional behavior and support use among Colobus angolensis palliatus of the Diani Forest, Kenya. *Primates* **56**, 183-192. doi:10.1007/s10329-015-0457-3

Fleagle, J. G., Stern, J. T., Jungers, W. L., Susman, R. L., Vangor, A. K. and Wells, J. P. (1981). Climbing: a biomechanical link with brachiation and with bipedalism. In *Symp Zool Soc Lond*, Vol. 48, pp. 359-375: Symposium Zoological Society London.

Frigon, A. (2017). The neural control of interlimb coordination during mammalian locomotion. *J. Neurophysiol.* **117**, 2224-2241. doi:10.1152/jn.00978.2016
Full, R. J. and Tu, M. S. (1991). Mechanics of a rapid running insect: two-, four-and six-legged locomotion. *J. Exp. Biol.* **156**, 215-231. doi:10.1242/jeb.156.1.215
Granatosky, M. C. and Schmitt, D. (2019). The mechanical origins of arm-swinging. *J. Hum. Evol.* **130**, 61-71. doi:10.1016/j.jhevol.2019.02.001
Higurashi, Y., Maier, M. A., Nakajima, K., Morita, K., Fujiki, S., Aoi, S., Mori, F., Murata, A. and Inase, M. (2019). Locomotor kinematics and EMG activity during quadrupedal vs. bipedal gait in the Japanese macaque. *J. Neurophysiol.* **122**, 398-412. doi:10.1152/jn.00803.2018
Hirasaki, E., Ogihara, N., Hamada, Y., Kumakura, H. and Nakatsukasa, M. (2004). Do highly trained monkeys walk like humans? A kinematic study of bipedal locomotion in bipedally trained Japanese macaques. *J. Hum. Evol.* **46**, 739-750. doi:10.1016/j.jhevol.2004.04.004
Hof, A. L. (1996). Scaling gait data to body size. *Gait Posture* **4**, 222-223. doi:10.1016/0966-6362(95)01057-2
Hunt, K. D. (1994). The evolution of human bipedality: ecology and functional morphology. *J. Hum. Evol.* **26**, 183-202. doi:10.1006/jhev.1994.1011
Hunt, K. D. (2016). Why are there apes? Evidence for the co-evolution of ape and monkey ecomorphology. *J. Anat.* **228**, 630-685. doi:10.1111/joa.12454
Hunt, K. D., Cant, J., Gebo, D., Rose, M., Walker, S. and Youlatos, D. (1996). Standardized descriptions of primate locomotor and postural modes. *Primates* **37**, 363-387. doi:10.1007/BF02381373
Isler, K. and Grüter, C. C. (2006). Arboreal locomotion in wild black-and-white snub-nosed monkeys (Rhinopithecus bieti). *Folia Primatol.* **77**, 195-211. doi:10.1159/000091229
Kimura, T. and Yaguramaki, N. (2009). Development of bipedal walking in humans and chimpanzees: a comparative study. *Folia Primatol.* **80**, 45-62. doi:10.1159/000209676
Kozma, E. E., Webb, N. M., Harcourt-Smith, W. E., Raichlen, D. A., D'Août, K., Brown, M. H., Finestone, E. M., Ross, S. R., Aerts, P. and Pontzer, H. (2018). Hip extensor mechanics and the evolution of walking and climbing capabilities in humans, apes, and fossil hominins. *Proc. Natl. Acad. Sci. USA* **115**, 4134-4139. doi:10.1073/pnas.1715120115
Maes, L. and Abourachid, A. (2013). Gait transitions and modular organization of mammal locomotion. *J. Exp. Biol.* **216**, 2257-2265.
Mori, S., Mori, F. and Nakajima, K. (2006). Higher nervous control of quadrupedal vs bipedal locomotion in non-human primates; Common and specific properties. In *Adaptive Motion of Animals and Machines*, pp. 53-65: Springer.
Myatt, J., Crompton, R. and Thorpe, S. (2011). A new method for recording complex positional behaviours and habitat interactions in primates. *Folia Primatol.* **82**, 13-24. doi:10.1159/000326795
Myatt, J. P. and Thorpe, S. K. S. (2011). Postural strategies employed by orangutans (*Pongo abelii*) during feeding in the terminal branch niche. *Am. J. Phys. Anthropol.* **146**, 73-82. doi:10.1002/ajpa.21548
Nakajima, K., Mori, F., Takasu, C., Mori, M., Matsuyama, K. and Mori, S. (2004). Biomechanical constraints in hindlimb joints during the quadrupedal versus bipedal locomotion of M. fuscata. In *Progress in Brain Research*, Vol. 143, pp. 183-190: Elsevier.
Nakajima, K., Mori, F., Takasu, C., Tachibana, A., Okumura, T., Mori, M. and Mori, S. (2001). Integration of upright posture and bipedal locomotion in non-human primates. In *Sensorimotor Control*, Vol. 326 (ed. R. Dengler and A. R. Kossev), pp. 95. IOS Press.
Nakatsukasa, M., Hirasaki, E. and Ogihara, N. (2006). Energy expenditure of bipedal walking is higher than that of quadrupedal walking in Japanese macaques. *Am. J. Phys. Anthropol.* **131**, 33-37. doi:10.1002/ajpa.20403
Ogihara, N., Makishima, H. and Nakatsukasa, M. (2010). Three-dimensional musculoskeletal kinematics during bipedal locomotion in the Japanese macaque, reconstructed based on an anatomical model-matching method. *J. Hum. Evol.* **58**, 252-261. doi:10.1016/j.jhevol.2009.11.009
Pontzer, H., Raichlen, D. A. and Rodman, P. S. (2014). Bipedal and quadrupedal locomotion in chimpanzees. *J. Hum. Evol.* **66**, 64-82. doi:10.1016/j.jhevol.2013.10.002
Preuschoft, H. (1989). Body shape and differences between species. *Hum. Evol.* **4**, 145-156. doi:10.1007/BF02435443
Preuschoft, H. (2004). Mechanisms for the acquisition of habitual bipedality: are there biomechanical reasons for the acquisition of upright bipedal posture? *J. Anat.* **204**, 363-384. doi:10.1111/j.0021-8782.2004.00303.x
Preuschoft, H. and Günther, M. (1994). Biomechanics and body shape in primates compared with horses. *Z. Morph. Anthropol.* **80**, 149-165.
Prost, J. H. (1965). A Definitional System for the Classification of Primate Locomotion. *Am. Anthropol.* **67**, 1198-1214. doi:10.1525/aa.1965.67.5.02a00060
Rose, M. (1976). Bipedal behavior of olive baboons (*Papio anubis*) and its relevance to an understanding of the evolution of human bipedalism. *Am. J. Phys. Anthropol.* **44**, 247-261. doi:10.1002/ajpa.1330440207
Rose, M. (1991). The process of bipedalization in hominids. In *Origine(s) de la bipédie chez les hominidés* (ed. C. Y and S. B), pp. 37-48. Paris: Editions du Centre National de la Recherche Scientifique.
Rosen, K. H., Jones, C. E. and DeSilva, J. M. (2022). Bipedal locomotion in zoo apes: Revisiting the hylobatian model for bipedal origins. *Evol. Hum. Sci.* **4**. doi:10.1017/ehs.2022.9
Sockol, M. D., Raichlen, D. A. and Pontzer, H. (2007). Chimpanzee locomotor energetics and the origin of human bipedalism. *Proc. Natl Acad. Sci. USA* **104**, 12265-12269. doi:10.1073/pnas.0703267104
Stanford, C. B. (2006). Arboreal bipedalism in wild chimpanzees: Implications for the evolution of hominid posture and locomotion. *Am. J. Phys. Anthropol.* **129**, 225-231. doi:10.1002/ajpa.20284
Thompson, N. E., Demes, B., O'Neill, M. C., Holowka, N. B. and Larson, S. G. (2015). Surprising trunk rotational capabilities in chimpanzees and implications for bipedal walking proficiency in early hominins. *Nat. Commun.* **6**, 8416. doi:10.1038/ncomms9416
Thompson, N. E., Rubinstein, D., Parrella-O'Donnell, W., Brett, M. A., Demes, B., Larson, S. G. and O'Neill, M. C. (2021). The loss of the 'pelvic step' in human evolution. *J. Exp. Biol.* **224**, jeb240440. doi:10.1242/jeb.240440
Thorpe, S. K. S. and Crompton, R. H. (2006). Orangutan positional behavior and the nature of arboreal locomotion in Hominoidea. *Am. J. Phys. Anthropol.* **131**, 384-401. doi:10.1002/ajpa.20422
Videan, E. N. and McGrew, W. C. (2001). Are bonobos (Pan paniscus) really more bipedal than chimpanzees (*Pan troglodytes*)? *Am. J. Primatol.* **54**, 233-239. doi:10.1002/ajp.1033
Videan, E. N. and McGrew, W. C. (2002). Bipedality in chimpanzee (*Pan troglodytes*) and bonobo (*Pan paniscus*): Testing hypotheses on the evolution of bipedalism. *Am. J. Phys. Anthropol.* **118**, 184-190. doi:10.1002/ajpa.10058
White, T. D., Lovejoy, C. O., Asfaw, B., Carlson, J. P. and Suwa, G. (2015). Neither chimpanzee nor human, Ardipithecus reveals the surprising ancestry of both. *Proc. Natl. Acad. Sci. USA* **112**, 4877-4884. doi:10.1073/pnas.1403659111
Wrangham, R. W. (1980). Bipedal locomotion as a feeding adaptation in gelada baboons, and its implications for hominid evolution. *J. Hum. Evol.* **9**, 329-331. doi:10.1016/0047-2484(80)90059-7
Young, N. M., Wagner, G. P. and Hallgrimsson, B. (2010). Development and the evolvability of human limbs. *Proc. Natl. Acad. Sci. USA* **107**, 3400-3405. doi:10.1073/pnas.0911856107
Zehr, E. P., Hundza, S. R. and Vasudevan, E. V. (2009). The quadrupedal nature of human bipedal locomotion. *Exerc. Sport Sci. Rev.* **37**, 102-108. doi:10.1097/JES.0b013e31819c2ed6
Zhu, W.-W., Garber, P. A., Bezanson, M., Qi, X.-G. and Li, B.-G. (2015). Age- and sex-based patterns of positional behavior and substrate utilization in the golden snub-nosed monkey (*Rhinopithecus roxellana*). *Am. J. Primatol.* **77**, 98-108. doi:10.1002/ajp.22314